Biogeosciences

Open Access

EGU

Forestlines in Italian mountains are shifting upward: detection and monitoring using satellite time series

Lorena Baglioni[1], Donato Morresi[2], Matteo Garbarino[3], Carlo Urbinati[1], Emanuele Lingua[4], Raffaella Marzano[3], and Alessandro Vitali[1]

[1]Department of Agricultural, Food and Environmental Sciences, Marche Polytechnic University, Ancona, Italy
[2]Department of Forest Resource Management, Swedish University of Agricultural Sciences, Umeå, Sweden
[3]Department of Agricultural, Forest and Food Sciences, University of Turin, Turin, Italy
[4]Department of Land, Environment, Agriculture and Forestry, University of Padua, Padua, Italy

Correspondence: Lorena Baglioni (lorena.baglioni@pm.univpm.it)

Abstract. The growing interest on the ecological effects of global warming and land use changes on vegetation, along with the development of remote sensing techniques, fostered applied research on the successional dynamics at the upper limits of forests. The aims of this study are (i) to develop an automated methodology for mapping the current position of the uppermost Italian forestlines and (ii) to identify hotspots of change by the analysis of long-term greenness and wetness spectral dynamics. We carried out a Landsat-based trend analysis in buffer zones along the forestlines, testing differences between sparse and dense canopy cover classes and at different elevations and distances to the forestline. We used regional-scale datasets and avoided to fix a minimum elevation threshold for the detection in order to make the method replicable in different mountain ranges. For the spectral dynamics analyses, we used Landsat time series of common vegetation indices for the period 1984–2023 and tested the significance of their long-term spectral trends with the contextual Mann–Kendall test for monotonicity. We determined that the highest forestlines are located in the western Alps for the Alps mountain range and in the central sector for the Apennines. We observed a general expansion of the forest cover mainly close to the forestline and at lower elevations. The highest values of greenness and wetness indices were, respectively, in the sparse tree cover class and in the dense one, particularly in the Alps.

1 Introduction

A treeline is the contiguous forest–grassland ecotone along an altitudinal or latitudinal gradient (Körner, 2008; Berdanier, 2010; Harsch et al., 2011). Nowadays, most treeline studies concern the response of spatio-temporal dynamics to climate and/or land use changes (Malanson et al., 2011). Current treeline elevation and its spatial patterns derive from air temperature increase and past human activities that have modified their physiognomy and dynamics over time (Holtmeier et al., 2005; Harsch et al., 2011). Most European mountain landscapes have been shaped since prehistoric times through fire, deforestation, and intensive grazing (Malanson et al., 2011; Vitali et al., 2018; Garbarino et al., 2020). In the Mediterranean region, the treeline elevation is much lower than its potential climatic position (Körner 2012; Piper et al., 2016). Moreover, human activities have locally altered, directly or indirectly, species composition (Obojes et al., 2024) and induced new disturbances as the in the western Alps, favoring *Larix decidua* Mill. to *Pinus cembra* L. and promoting an invasive resprouter like *Alnus viridis* (Chaix) DC. (Motta et al., 2006; Dziomber et al., 2024). In the Apennines, *Pinus nigra* J.F. Arnold plantations at higher elevations facilitated its upward encroachment in treeline ecotones (Vitali et al., 2017). The upward treeline shift occurring in many parts of the globe can therefore be associated with not only global warming (Hansson et al., 2023) but also successional dynamics (Ameztegui et al., 2016; Vitali et al., 2017) and geomorphic processes (Leonelli et al., 2009).

The development of remote sensing techniques and geographic information systems provided new opportunities in treeline studies (Holtmeier et al., 2020) such as detecting and monitoring the dynamic patterns of treeline shape and density (Fissore et al., 2015). Defining clear and easily replicable methods based on the application of modern technologies to access available datasets is fundamental for accurate and large-scale treeline monitoring. At the local scale, aerial photography is commonly used (Ameztegui et al., 2016; Hansson et al., 2020; Nguyen et al., 2024) since it provides older images than satellite ones, although image quality and availability are limiting factors (Morley et al., 2018). At larger scales, He et al. (2023) detected closed-loop mountain treelines integrating high-resolution tree cover maps and digital elevation models, whereas Wei et al. (2020) in the western United States proposed an "alpine treeline ecotone detection index" (ATEI) based on the analysis of altitudinal and normalized difference vegetation index (NDVI) gradients. At the regional scale, supervised and unsupervised classification of multispectral images are widely used (Fissore et al., 2015; Chhetri and Thai, 2019), as well as detection techniques based on land cover maps combined with digital elevation models (e.g., Pecher et al., 2011).

Besides mapping, current treeline research includes also its spatio-temporal dynamics. Despite the coarser spatial resolution and the limitation of cloud cover, satellite optical imagery offers a finer time resolution by integrating data from several platforms and free processed time series. It also provides spectral information for synchronic analysis of vegetation changes (Gómez et al., 2016). The free access to its database in 2008 has increased the use of Landsat time series (Zhu, 2017). Given their spatial resolution (30 m) and temporal data availability, Landsat images have been largely used for vegetation dynamics monitoring, such as post-disturbance forest recovery (Morresi et al., 2019) and greening or browning in different ecosystems (Kumar et al., 2022; Rumpf et al., 2022; Bayle et al., 2024), and to study alpine treelines by applying greening proxies like vegetation indices (Fissore et al., 2015; Tian et al., 2022). The NDVI is widely used in treeline dynamics monitoring, being more sensitive in detecting biomass changes in open rather than in closed canopies (Bharti et al., 2012; Arekhi et al., 2018; Wei et al., 2020; Choler et al., 2021; Zou et al., 2022; Bayle et al., 2025). In the European Alps, Carlson et al. (2017) and Choler et al. (2021) used the annual peak values of NDVI (NDVI-max) to analyze the greening trends from Landsat and MODIS time series. They assessed a significantly increasing spectral trend over the last 2 decades, mainly at north-facing slopes and in sparsely vegetated areas. Nevertheless, Bayle et al. (2024) remarked that the higher number of Landsat observations throughout the growing seasons can affect the NDVI-max trend analysis, causing false outcomes. It is true that annual NDVI-max increase with the number of available observations, and therefore their frequency must be taken into account. In the southwestern part of the European Alps, Bayle et al. (2025) studied greening trends using the annual max of the kernel normalized difference vegetation index (kNDVI) (Camps-Valls et al., 2021), a nonlinear version of the NDVI, overcoming the overestimation of greening by the harmonic analysis of time series (HANTS), as reported by Choler et al. (2024). Bolton et al. (2018), instead, used the enhanced vegetation index (EVI) for a Landsat-based greening trend analysis of alpine treelines in the Canadian boreal zone. The EVI corrects the aerosol influence and canopy background noise, and it is less affected by saturation than NDVI, being more sensitive to the near-infrared (NIR) band (Huete et al., 2012). For this reason, it can detect the spectral behavior of lower layers of vegetation, while the NDVI responds mainly to the RED band, which is involved in photosynthetic activity of the upper canopy layer. A single index can be combined with other vegetation indices to reduce the uncertainty in change detection analysis (Schultz et al., 2016; Zhou et al., 2023). EVI and NDVI can be considered greenness indices since they are linked to the photosynthetic activity of vegetation using NIR and RED bands, while wetness indices introduce shortwave infrared (SWIR) bands that are especially sensitive to the water content of vegetation (Huete, 2012). Examples of wetness indices are the normalized difference moisture index (NDMI) and the normalized burn ratio (NBR) index. Such indices are sensitive to shadowing, forest structure, leaf internal structure, vegetation moisture and density (Schroeder et al., 2011). In Landsat-based forestry applications, indices derived from the tasseled cap transformation (TCT) (Kauth and Thomas, 1976; Crist and Cicone, 1984) are also commonly used, since they are less affected by soil reflectance (Cohen and Goward, 2004). The tasseled cap wetness index (TCW) considers the visible bands and both SWIR1 and the SWIR2, and it is suitable to predict forest structural attributes, being slightly influenced by topographic variations, especially in closed conifer stands (Cohen et al., 1995). Another TCT index is the tasseled cap angle (TCA) (Powell et al., 2010), combining the greenness and brightness information as defined in Crist and Cicone (1984) to assess the ratio between vegetated and non-vegetated areas (Gómez et al., 2011). In this study, we consider the "forestline" to be the line separating the closed forest from the shrubland and grassland above and the "treeline" or "forestline ecotone" to be the surrounding area, the spatial pattern of which was not investigated due to the scale of analysis adopted. Forestline ecotones are dynamic ecosystems, and their monitoring at regional scale can be conducted with the analysis of their spectral behavior over time adopting different indices and tools. In this context, our study analyzed forestline dynamics of the two main Italian mountain ranges, the Alps and the Apennines. Our research aims were

1. to define and monitor the position of the uppermost forestlines with an automated methodology;

2. to identify hotspots of change through satellite data, verifying whether and where forest recolonization dynamics are occurring.

In particular, we analyzed the long-term greenness and wetness spectral changes of the uppermost forests and the contiguous forestline ecotones using a Landsat-based trend analysis of time series for the period 1984–2023, and we tested if greenness and wetness indices trends differed with elevation, forestline distance, and canopy cover densities. We hypothesized that greenness indices are more fitted for forest recolonization of open areas, while wetness indices are better suited for detecting gap-filling processes by intercepting also the spectral signal of lower leaf strata.

2 Materials and methods

2.1 Study area

The Alps and the Apennines are the two major mountain ranges of the Italian peninsula. They extend, respectively, for 1300 and 1350 km: the Alps from west to east across northern Italy; the Apennines from the northwest to the southeast. They differ in climate, elevation range, and vegetation characteristics. In the Alps, annual precipitation ranges between 400 and 3000 mm, with rare summer dry periods and cold winters (Isotta et al., 2014). Conifer forests prevail in the subalpine zone, where the main species are Norway spruce (*Picea abies* (L.) H. Karst.), European larch (*Larix decidua* Mill.), and Swiss stone pine (*Pinus cembra* L.) (Fauquette et al., 2018). In the Apennines, the total annual precipitation ranges between 600 and 4500 mm (Vacchiano et al., 2017), with short and pronounced summer dry periods (Blasi et al., 2014). Mixed broadleaf forests dominate at lower elevations, while common beech (*Fagus sylvatica* L.), locally mixed with silver fir (*Abies alba* Mill.), is the main species in the montane zone, except for rare locations in the central and southern Apennines, where also mountain pine (*Pinus mugo* Turra), European black pine (*Pinus nigra* J. F. Arnold), and Bosnian pine (*Pinus heldreichii* H. Christ) occur naturally. With the Italian forestline ecotones being the target of our study, we selected the highest peak for each mountain group of the Alps and of the Apennines, as defined by the Global Mountain Biodiversity Assessment (GMBA) inventory (Snethlage et al., 2022a, b). We located the exact position of the peaks using the nationwide Tinitaly digital elevation model (DEM) v 1.1 (Tarquini et al., 2023) that is a DEM with a 10 m spatial resolution obtained from the union and harmonization of each Italian administrative regions' digital terrain models. We then filtered the mountain groups and retained only the ones with the highest peaks located on bare soil or in snow-/ice-covered areas according to the Dynamic World land cover map (Brown et al., 2022). In this way, we excluded also the mountain groups completely covered by forest or affected by severe human im-

pacts, such as urbanized areas or areas with settlements. In addition, for excluding the mountain peaks lacking the alpine belt thermoclimatic features, we used the oro-temperate, cryo-oro-temperate, and gelid thermotypes derived from the Bioclimates of Italy dataset (Pesaresi et al., 2017) based on the Worldwide Bioclimatic Classification System (WBCS) by Rivas-Martínez (1993). Other GMBA mountain groups have been removed after the previous selection based on land cover and bioclimatic parameters because the Italian administrative and GMBA's boundaries limited the altitudinal range and forest distribution of some groups on the border in the following analyses (Sect. 2.2).

2.2 Detection of forestlines

We used the Tree Cover Density 2018 (TCD) dataset of the European Environment Agency (EEA) derived from Sentinel-2 multispectral data as a reference for forest cover (Copernicus Land Monitoring Service, 2024). TCD has a 10 m spatial resolution and provides information about the percentage of crown coverage in each pixel with a minimum thematic target producer and user accuracies of 90 % (EEA, 2025). According to the FAO "forest" definition (FAO, 2000), we selected only pixels with a TCD higher than 10 % to obtain a mask of forested areas. For each mountain group, we obtained the vertical distance between each forest pixel and the DEM-derived highest peak. We then selected the forest pixels with a vertical distance within the first percentile of all the distances and extracted the contours of the forestline by considering only the side of each selected forest pixel facing the mountain peak. We avoided a minimum elevation threshold for the forestline detection to facilitate the replicability of the method in geographic regions with different altitudinal ranges. We joined polylines with linear gaps shorter than 30 m (corresponding to the Landsat spatial resolution). We considered only resulting polylines longer than 500 m to avoid highly fragmented forestlines and to focus on more spatially extended and continuous ecotones, and we removed closed loops to exclude the edges of forest gaps below the forestline. We defined a buffer zone of a 250 m radius (Fig. 1c) along the forestlines to assess the presence of significant spectral changes in a gradient from closed forest to grassland. We also sampled points at 10 m intervals along the detected forestlines to assess the mean, median, and maximum elevation of all of them clustered by mountain groups or ranges. We processed the data in the R software environment (v. 4.3.2), using the "terra" (Hijmans, 2023), "callr" (Csárdi and Chang, 2024), and "future.apply" (Bengtsson, 2021) packages, and with QGIS software (v. 3.34.1).

2.3 Trend analysis of vegetation indices

Sentinel-2 provides images with a higher spatial resolution (10 m) but a shorter time span (since 2018) than Landsat. In fact, Landsat images have supplied multispectral informa-
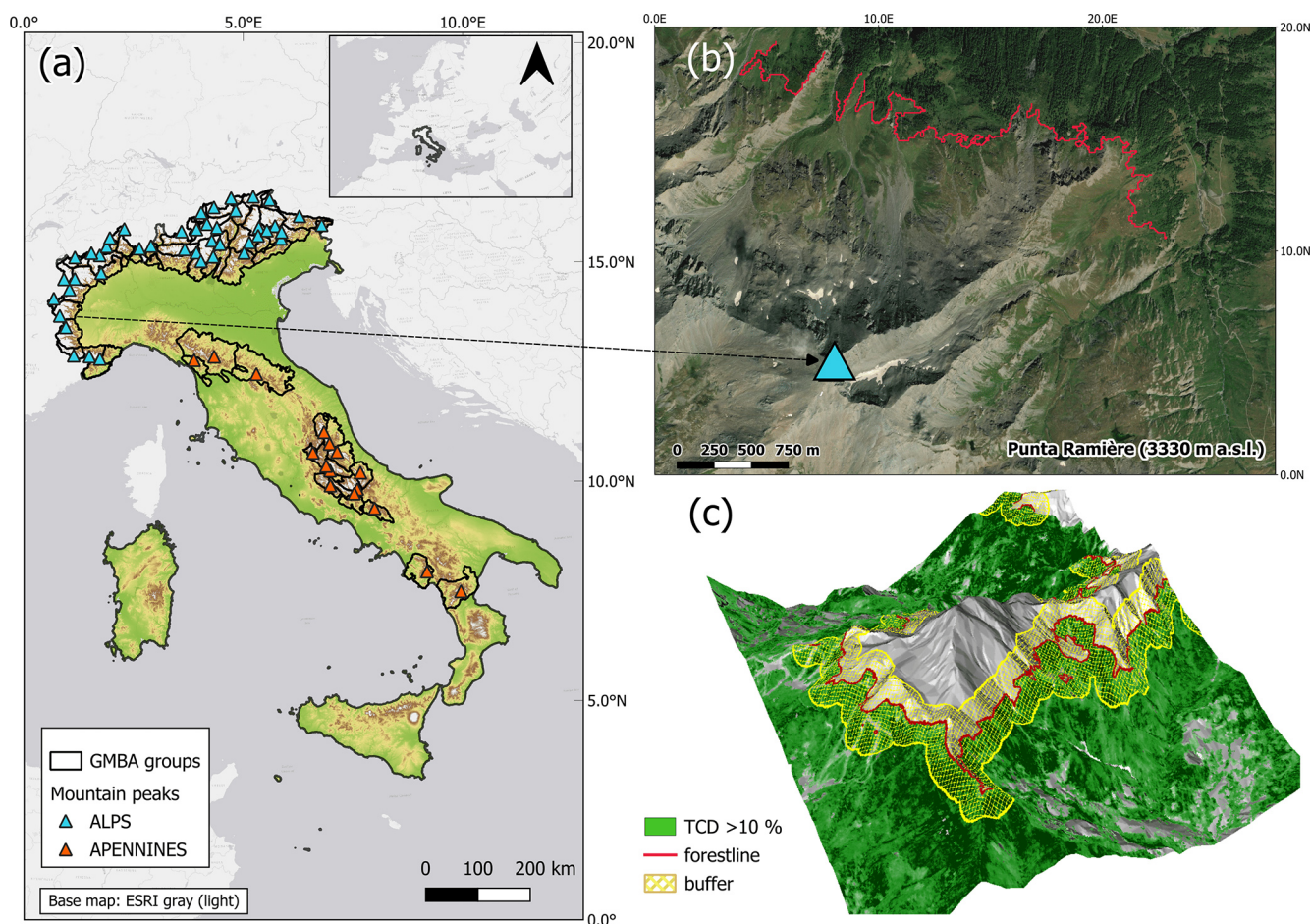
Figure 1. (a) Selected peaks (triangles) along the Italian Alps (light blue) and the Apennines (orange). **(b)** Detected forestlines (red polylines) on an ESRI satellite image (ArcGIS/World_Imagery) of Punta Ramière (3330 m a.s.l.) in the Montgenèvre Alps GMBA group. **(c)** a 3D graphical model based on the Tinitaly DEM and the TCD forest mask (TCD >10 %) used for the forestline detection and the buffer area definition (yellow area).

tion at medium resolution (30 m pixel size) since 1984 and are commonly used in treeline studies (Bharti et al., 2012; Arekhi et al., 2018; Morley et al., 2019; Garbarino et al., 2023) since they give a good compromise between space and time resolution at regional scale (Hansson et al., 2020). We collected Landsat images acquired from 1 June to 30 September of each year in the period from 1984 to 2023 to analyze forest vegetation dynamics during the growing season. In particular, we used Level-2 Collection 2 Landsat images acquired by the TM, ETM+, OLI, and OLI-2 sensors. After masking pixels covered by snow, clouds, cloud shadows, and water, we produced pixel-based reflectance composites based on the medoid compositing approach (Flood, 2013). We preferred the medoid technique over the traditional compositing approaches because it is more robust to outliers and noise. In fact, it consists of the closest value to the median. We computed common vegetation indices from reflectance composites that we grouped into (i) greenness indices – normalized difference vegetation index (NDVI) (Tucker, 1979), en-

hanced vegetation index (EVI) (Huete et al., 2002), and tasseled cap angle (TCA) (Powell et al., 2010) – and (ii) wetness indices – normalized burn ratio (NBR) (García et al., 1991), normalized difference moisture index (NDMI) (Gao, 1996), and tasseled cap wetness (TCW) (Crist, 1985). Finally, we masked the 40-year-long time series using the buffer areas around each selected forestline (Sect. 2.2).

We assessed the significance in the monotonicity of the spectral trends, i.e., strictly increasing or decreasing, derived from vegetation indices time series by applying the nonparametric contextual Mann–Kendall (CMK) statistical test (Neeti et al., 2011). The CMK test is an estimator of the monotonicity of trends based on the Mann–Kendall (MK) test, which takes into account the trends in the neighboring pixels within a 3×3 kernel. In this way, the spatial autocorrelation is considered, thus improving the detection of spatial patterns characterized by homogeneous spectral trends. Specifically, we used the ConMK R package (Rajala, 2024). The TAU statistics produced by the MK test ranges between

+1 and −1, with positive values indicating an increasing trend, while negative values are associated with decreasing trends. Before checking the occurrence of significant trends by computing the p value (α) associated with the TAU statistics, we pre-processed time series in two steps. Firstly, we filled 1-year data gaps at the pixel level through linear interpolation while discarding pixels with longer data gaps. Secondly, we removed the autocorrelation in the time series by applying the "pre-whitening" procedure proposed by Wang and Swail (2001) and implemented in the ConMK R package.

2.4 Assessment of the spectral trends

For each group of vegetation indices, i.e., greenness and wetness, we selected only those pixels that exhibited a highly significant trend ($\alpha < 0.005$), as proposed in Choler et al. (2021) for all the indices (Fig. 2).

We used the points corresponding to the resulting pixel centroids to extract the mean TAU value among the vegetation indices and the elevation from the Tinitaly DEM. The original TCD excludes shrublands, dwarf pine, or green alder in alpine areas (EEA, 2025), but we resampled it to 30 m by average and assigned to each pixel centroid also the mean tree canopy cover. We excluded points with negative trends (TAU < 0), and with TCD = 0, that corresponded to areas without a tree canopy cover (e.g., grasslands) and where the significant increasing spectral trend of the last 40 years was probably due to factors and dynamics different from forest recolonization. We assigned the elevation value of the nearest forestline point to the resulting wetness and greenness points using the "join attributes by nearest" tool in QGIS. In this way, we obtained the Euclidean distance of each trend point to the forestline and the elevation difference, which we used to classify the points above or below the forestline. In particular, we identified the relative position of each point to the forestline by multiplying the Euclidean distances by the sign of the elevation difference. We carried out the analysis separately for the Alps and the Apennines given their altitudinal, climatic, and vegetation differences. After this characterization of the trend points, we randomly sampled two sets of 40 000 points for each mountain range by the "slice_sample()" function of the "dplyr" R package (Wickham et al., 2023). Each set contained an equal number of greenness and wetness significant trend points. We then grouped the sampled points into three tree canopy cover categories according to TCD: (i) sparse canopy cover (TCD < 10 %), (ii) moderate to dense canopy cover (10 % < TCD < 80 %), and (iii) dense canopy cover (TCD > 80 %). Because of the large canopy cover classes ranges to which the points were allocated taking into account a mean TCD value, a possible spatial mismatch between the resampled TCD and the Landsat data was ignored. We then assessed the relationship between TAU values and the canopy cover, the elevation, and the distance to forestline, taking into account the mean values of each forestline segment. We used a Wilcoxon test (Wilcoxon, 1945) to verify significant differences between the mean TAU among wetness and greenness indices, averaging the mean TAU values of each canopy cover class in each forestline buffer. Finally, we built generalized additive models (GAMs) (Hastie and Tibshirani, 1990) using the cubic spline smoother of the "mgcv" R package (Wood, 2011) to test the presence of a significant nonlinear relationship between the mean TAU values and (i) the elevation and (ii) the forestline distance without considering the TCD classes.

3 Results

3.1 Forestline extraction

We identified and processed 60 mountain peaks, 44 in the Alps and 16 in the Apennines (Table A1, Appendix A). We obtained approximately 5760 km of forestlines with a mean elevation of 2088 ± 193 m a.s.l. in the Alps and 1758 ± 161 m a.s.l. in the Apennines, with a maximum elevation, respectively, of 2500 and 2383 m a.s.l. In the Alps, the lowest forestline elevations were in the prealpine groups due to the lack of a suitable altitudinal gradient, whereas the highest ones were mainly in the western sector (Fig. 4a). In the Apennines, the lowest and less extended forestlines, if compared to the forested areas, were in the northern sector, while the highest ones were in central Italy: the Majella (MJ), Sirente Velino (SVE), and Marsicani (MM) mountain groups (Fig. 4b). The total area of interest extended approximately for 1880 km^2.

3.2 Trend analysis and performances

We obtained 28.81 % of highly significant ($\alpha < 0.005$) trend pixels for greenness and 19.69 % for wetness, considering only pixels with concordant p values on all of the indices. The majority of TAU values were positive (Fig. 5) at both index types, with, respectively, 97.8 % and 99.8 % in the Alps and 96.3 % and 99.7 % in the Apennines.

In total, we obtained 242 233 greenness and 221 554 wetness highly significant positive trend pixels for the Alps and 76 348 and 508 745, respectively, for the Apennines. With sparse and moderate to dense canopy cover, the greenness and wetness positive trends were mainly near the forestline in both mountain ranges and decreased in both directions, but mainly upward where tree-covered areas are gradually replaced by high-altitude grasslands. With dense canopy cover, only wetness positive trends in the Apennines showed a similar distribution, differently from greenness trends and from both types in the Alps, where the highest concentration was below and distant from the forestline (Fig. 6).

Significant differences between TAU trends and canopy cover classes occurred mainly in the Alps (Fig. 7). The highest ones were for the wetness indices in the dense canopy
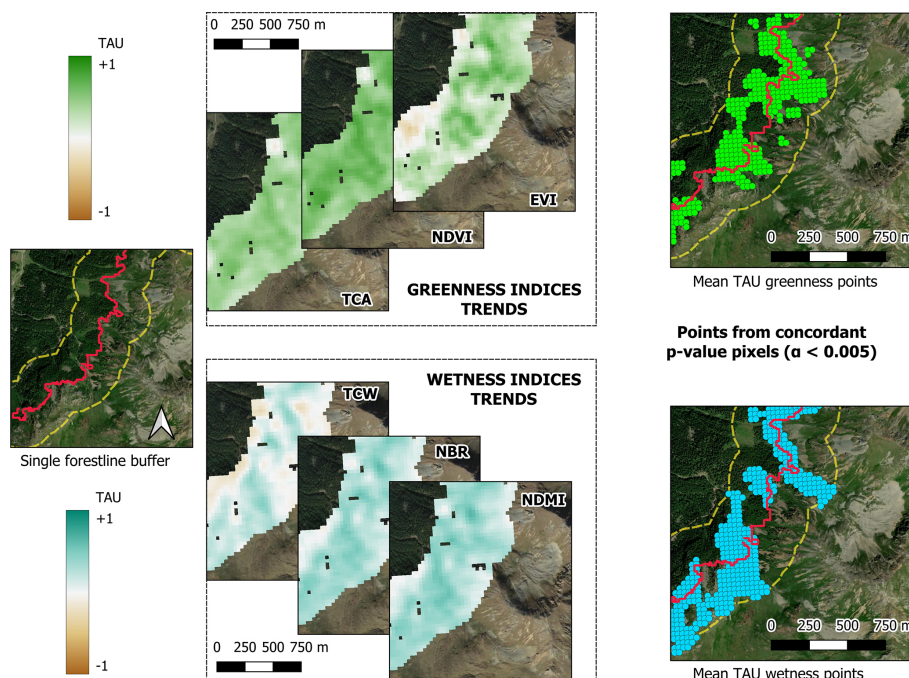
Figure 2. Example of the extraction of the highly significant ($\alpha < 0.005$) greenness (top) and wetness (bottom) points trends in the buffer area (yellow dotted line) around a single forestline (full red polyline) in the Alps. Base map: ESRI Satellite (ArcGIS/World_Imagery).
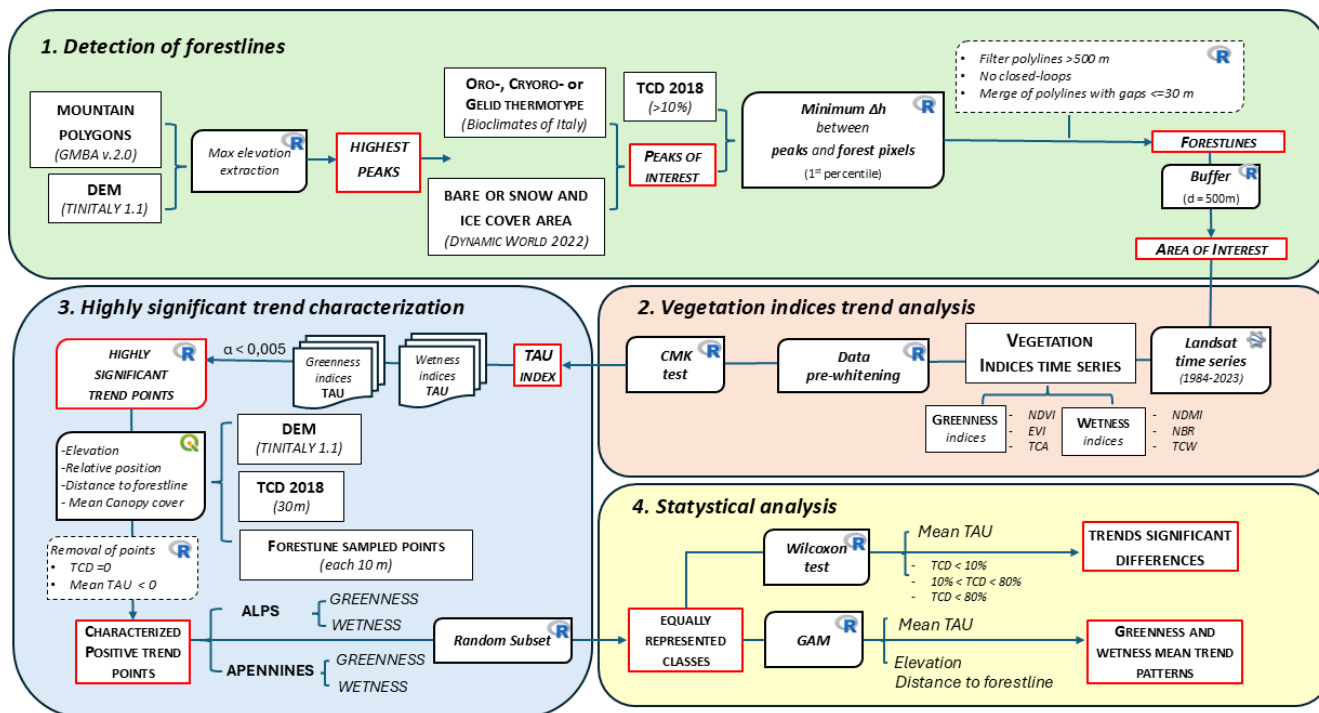

Figure 3. Flow chart of the analytical process: input data (black rectangles), outputs (red rectangles), and statistical analyses (irregular rectangles). Abbreviations: DEM (digital elevation model), TCD (tree cover density), NDVI (normalized difference vegetation index), EVI (enhanced vegetation index), TCA (tasseled cap angle index), NDMI (normalized difference moisture index), NBR (normalized burn ratio), TCW (tasseled cap wetness), CMK (contextual Mann–Kendall test), and GAM (generalized additive model).
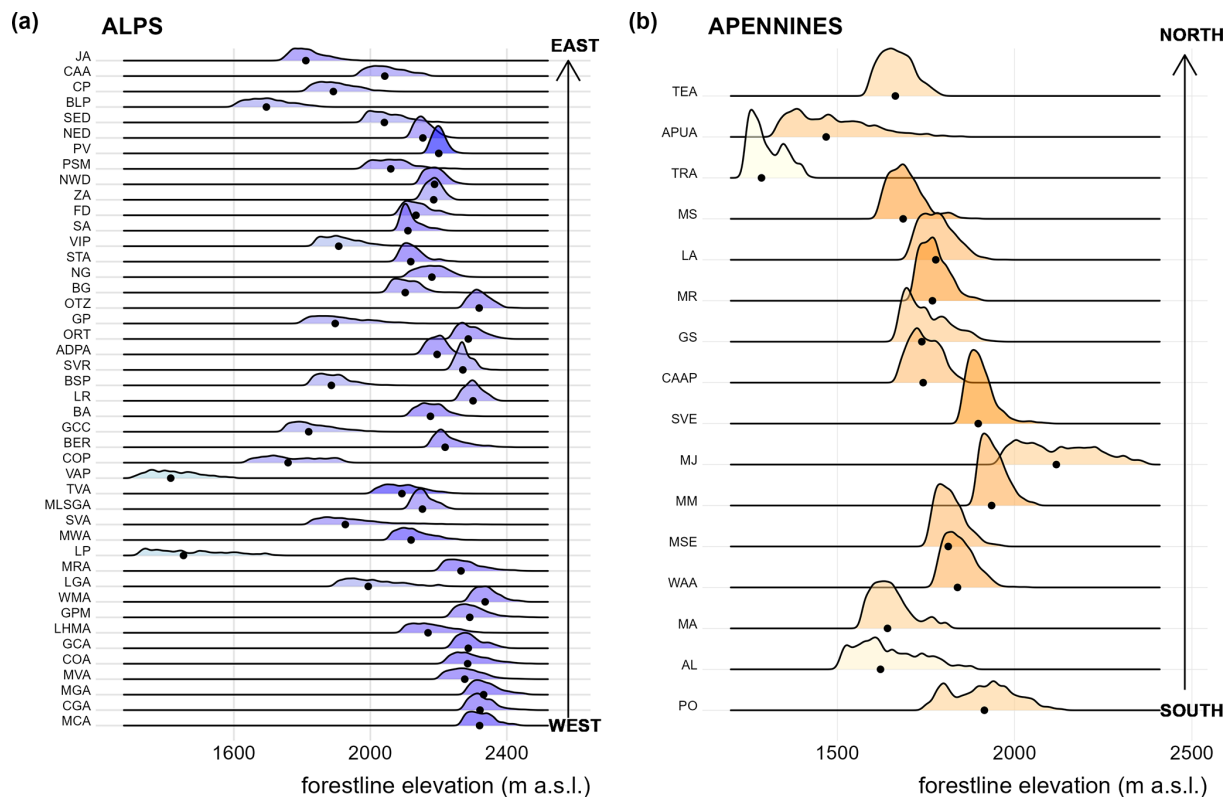
Figure 4. (a) Forestline elevation ranges of the mountain groups in the Alps ($n = 44$) sorted by longitude (west–east). **(b)** Forestline elevation ranges of the mountain groups of the Apennines ($n = 16$) sorted by latitude (south–north). Black dots are the median values of each interval; the color intensity of ridges increases with forestline length and forested area ratio. Mountain group codes are available in Table A1 (Appendix A).

cover. For greenness, sparse canopy cover class had a higher mean TAU than moderate to dense and dense classes. In the Apennines, only greenness values highlighted a significant difference between the sparse and the dense canopy cover class.

GAMs did not detect a statistically significant relationship between the greenness/wetness mean TAU values, the distance to forestline, and the elevation (Fig. 8). This result is probably due to the fact that a combination of topographic, climatic, and anthropogenic drivers must be considered to assess what are the main drivers of these spectral trends, taking into account the main differences between the Alps and the Apennines. Relatively similar patterns of the two index mean trends appeared at both mountain ranges but had a higher variability in the Apennines. In general, TAU greenness values were higher than wetness ones. In the Alps, greenness increased moving upward to the forestline with a first culmination close to and below it followed by a decrease and another increase, with the highest mean values being over 200 m. In the Apennines instead, the mean TAU values increased close to the forestline with a culmination above it (about 100 m distance) and were followed by a decrease, with the lowest values being above 200 m. In both mountain ranges, we ob-

served a decrease in the greenness trends from lower elevations up to about 1750 m a.s.l. in the Alps and 1500 m a.s.l. in the Apennines (Fig. 8b). Thereafter, the mean TAU values increase progressively in the Alps up to 2300 m a.s.l., but decrease slightly in the Apennines to around 1700 m a.s.l. to rise again up to the altitudinal limit.

The wetness trend related to the forestline distance is very flat in the Alps and relatively similar to that of the greenness, whereas in the Apennines, the trend is far more variable and increasing progressively from the forestline to 200 m above it (Fig. 8a). Wetness curves decrease for both Alps and Apennines from the lower elevations to about 1600 m a.s.l (Fig. 8b), with a more pronounced slope for the Apennines. Then they both rise up to about 2100 m a.s.l. with a steeper and fluctuating trend again in the Apennines.

4 Discussions

4.1 The uppermost forestline detection method

The proposed forestline detection method is applicable at different spatial scales and in different geographic regions as it does not establish elevation thresholds and it can be
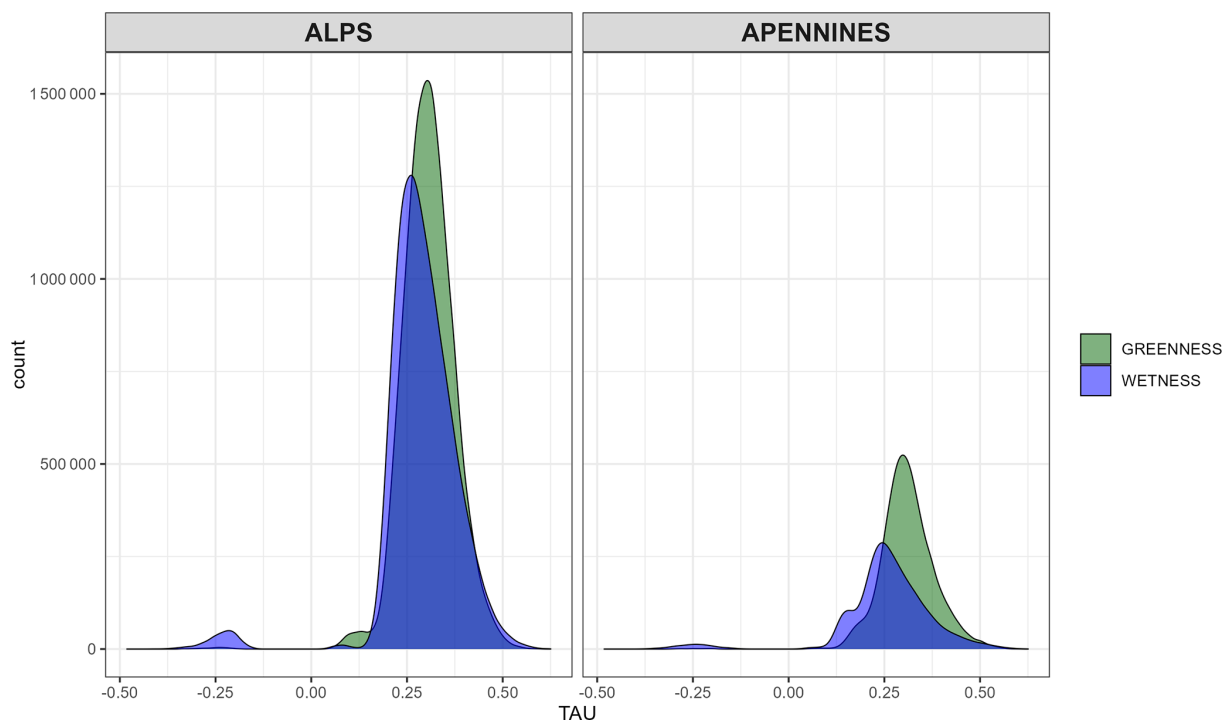
Figure 5. Distribution of the highly significant ($\alpha < 0.005$) wetness (blue) and greenness (green) pixel frequency with different TAU values.

based on regional datasets or other existing digital elevation models and forest masks. In addition, the method is also not exclusively based on climatic parameters; therefore, it is applicable for the detection of human-impacted forestlines. We considered forestlines closer to their potential climatic limit (e.g., tree species line), excluding forest margins at lower elevations and highly fragmented forestlines. We based the detection on the smallest elevation differences between the highest peaks and the forested pixels resulting from recent satellite-derived data (TCD). According to some authors, Italian and many other Northern Hemisphere forestlines could not be considered "climatic" treelines for their severe human constraints (e.g., grazing, fire, and deforestation) that altered altitudinal position, spatial patterns, and tree composition (Motta et al., 2006; Malanson et al., 2011; Piermattei et al., 2016; Vitali et al., 2018; Holtmeier and Broll, 2020). In Italian mountains, forest upward expansion was favored mainly by past large-scale disturbances and took place mainly at warmer aspects (Malandra et al., 2019). Recurrent human direct impacts on these ecotones since the Holocene times have greatly affected vegetation structure and composition (Foster et al., 1998), and recent silvo-pastoral abandonment at high-elevation sites triggered secondary succession (Debussche et al., 1999). The different forest cover and the bioclimatic features of the selected mountain groups provide a representative sample of the forestline trends along the Italian Peninsula. The mean forestline elevations detected confirm previous studies in the Alps (Caccianiga et al., 2008; Lingua et al., 2008; Diàz-Varela et al., 2010; Gilles et al.,

2023) and in the Apennines (Vitali et al., 2018; Bonanomi et al., 2020). However, since the proposed method is closely dependent on the available regional/national datasets, some exclusion occurred with mountain groups at transnational borders.

4.2 Long-term greenness and wetness spectral trends

Overall, rising greenness and wetness trends were recorded at both mountain ranges in line with the ongoing natural reforestation processes (Vitali et al., 2018; Garbarino et al., 2020; Anselmetto et al., 2022). Pixel density distribution in the Alps and Apennines is globally very similar, but some differences occur for the dense canopy cover class in the Apennines, where the wetness indices have the highest trend peak just below the forestline. This could be attributed to the different species composition at the two mountain ranges. Along the Apennines, with the exception of some scattered locations with *Pinus*, *Fagus sylvatica* is practically the only upper-forestline species (Piermattei et al., 2014; Vitali et al., 2017). This would confirm the long-term impact of human activity (Körner, 2012) and explain the occurrence of "abrupt" (Harsch et al., 2011) and static treelines (Bonanomi et al., 2018; Bader et al., 2021) given the very limited seed dispersal efficiency of beech (Vitali et al., 2017). Dominant species colonization rates, reproduction, seed-dispersal strategy, and vitality of the occurring species are relevant issues when comparing forestlines shifts in the Alps and Apennines (Holtmeier, 2009; Compostella et al., 2017; Garbarino et al.,
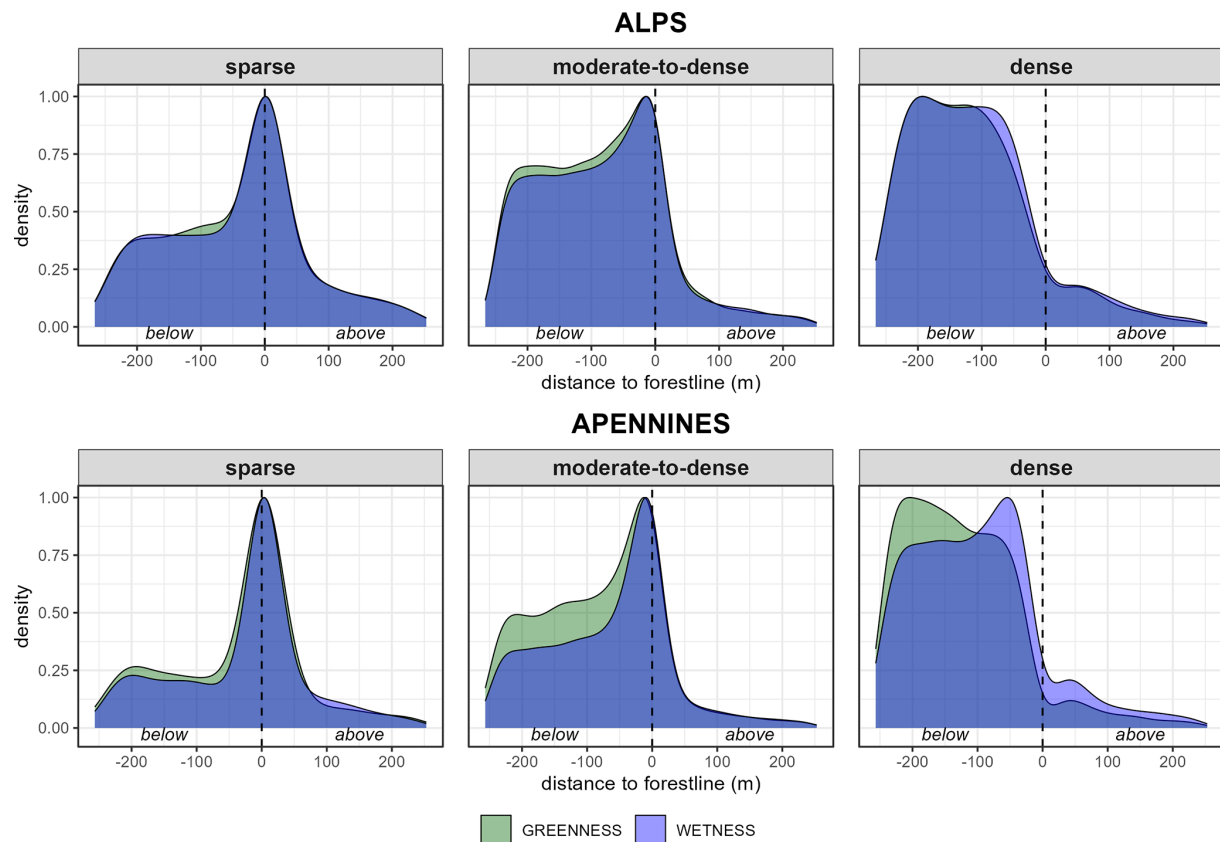
Figure 6. Positive wetness (blue) and greenness (green) trend pixel density according to their distance to the forestline (black dashed line) in different canopy cover classes: sparse (TCD < 10 %), moderate to dense (10 % < TCD < 80 %), and dense (TCD > 80 %). Negative and positive values represent distances below and above the forestline, respectively.

2020). In general, gap-filling processes prevail at the deciduous Apennine forestlines (Malandra et al., 2019; Vitali et al., 2018), whereas in the Alps the coniferous treeline species (e.g., *Larix decidua*, *Pinus cembra* and *Picea abies*) are more prone to tree encroachment at higher elevations. In the Apennine abrupt treelines, the beech regeneration (by seeds and suckers) have favored processes of canopy thickening and gap filling below and near the forestline, better intercepted by wetness indices that are more sensitive to the spectral response of the less exposed vegetation. Wetness indices are particularly sensitive to water content in both soil and plants especially in canopy leaf tissues. For this reason, we believe that significant increasing trends in areas with a dense canopy cover could be associated with crown thinning and biomass increase, as in gap filling, while in areas with sparse canopy cover, they could be associated with new encroachment in open areas.

Taking into account the magnitude of changes rather than their frequency, in the Apennines, we found a significant difference only for greenness mean TAU, lower in dense rather than in sparse canopy cover conditions. We assume that the drier climate of the Apennines may have influenced the positive trends of wetness indices, reducing the TAU variabil-

ity in different canopy classes. The Wilcoxon test revealed the most significant variations in the Alps, where summer drought is not a limiting factor as in the Apennines. This hypothesis is confirmed by the higher mean TAU values of greenness in the sparse canopy class, whereas those of wetness refer to the dense one. Carlson et al. (2017) in the French Alps found a stronger greening signal in low shrubs and open areas (e.g., grasslands or rocky habitats) than in forested areas. As well McManus et al. (2012) in the forest–tundra ecotones in Canada found higher greening in shrub and grass canopy classes. Sometimes, the greening of sparse open areas may be affected by melting glaciers (Rumpf et al., 2022), inducing a possible increase in soil moisture and influencing wetness trends too. Without considering the canopy cover class, the most relevant changes in the Apennines occurred above the forestline and at the lowest (<1500 m a.s.l.) and highest (>2000 m a.s.l.) elevations. Further information about the forest structure could help detecting if the spectral signal sourced mostly from shrubs or newly established trees. In the Apennines, the highest mean TAU values above the forestline can be due to species such as *Juniperus communis* L., *Pinus mugo* Turra, and *Vaccinum mirtillus* L. that facilitate the upward migration of beech trees (Bonanomi et
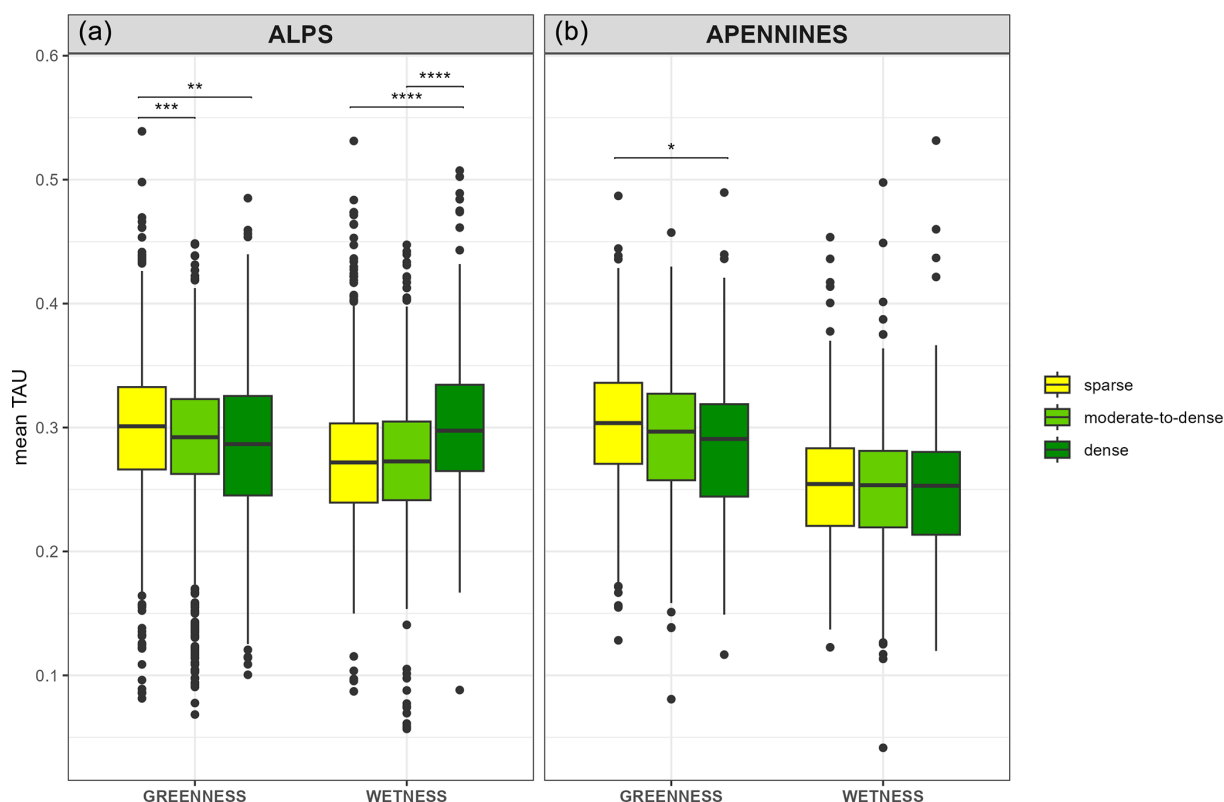
Figure 7. Boxplots of the mean TAU values of wetness and greenness trends in the Alps **(a)** and in the Apennines **(b)**. The mean values in each forestline buffer account for three different canopy cover classes: sparse (yellow), moderate to dense (green), and dense (dark green). Significant differences between Wilcoxon tests are indicated with * ($\alpha \leq 0.05$), ** ($\alpha \leq 0.01$), *** ($\alpha \leq 0.001$), and **** ($\alpha \leq 0.0001$). For more information on the canopy cover classes percentage in the Alps and in the Apennines, refer to Fig. B1 (Appendix B).

al., 2021). In the Alps, we found a steadier increase in TAU greenness and wetness from below to above the forestline. This confirms that diffuse treelines are more common in the Alps (Garbarino et al., 2020). Some authors used lidar data from the Global Ecosystem Dynamics Investigation (GEDI), integrated with Landsat and Sentinel-2 data (Potapov et al., 2021; Tolan et al., 2024; Lang et al., 2023) to assess canopy height, vertical canopy structure, and surface elevation with the aim of monitoring forest ecosystems and carbon fluxes. This approach could be adopted in monitoring ecotones such as treelines (Bolton et al., 2018) and also to predict future vegetation scenarios and provide suitable management options (Morales-Molino et al., 2022).

Considering the greenness and wetness mean values of TAU trends only as a function of elevation, without the forestline distance information, their higher values are mainly at lower sites, where temperature is less limiting and the past human impact was greater (Malandra et al., 2019; Anselmetto et al., 2022). Furthermore, forests at lower elevations are more accessible and usually have been most intensively managed in the past, although they now are largely abandoned (Malandra et al., 2019; Garbarino et al., 2020). Above the mean forestline elevation of both the Alps and

Apennines, the mean TAU values increase and then decrease at higher altitudes where the number of pixels with significant increasing trends is also lower. In the Apennines, a second short but clear decrease above 1750 m a.s.l. may depend on the frequent abrupt beech treelines where the forest margin is sharply separated from areas with sparse and different vegetation. This common trend for both mountain ranges confirms an upward recolonization process at the Italian anthropogenic treelines. The decreasing magnitude observed at a higher elevation with the increasing distance from the forestline is probably due to the larger distance from seed trees (Vitali et al., 2018), the more limiting effect of temperature, and the synergic effect of topography and microclimate.

Uncertainty remains about what caused the spatial variability of trends, as noted also by Choler et al. (2021). The time series span and the spatial resolution of satellite images are crucial items in the definition of these ecological models. Nevertheless, the integration of different data sources (e.g., lidar) and the modeling of further environmental, climatic, and anthropogenic drivers can be useful for a better understanding of the current and future forestline dynamics.
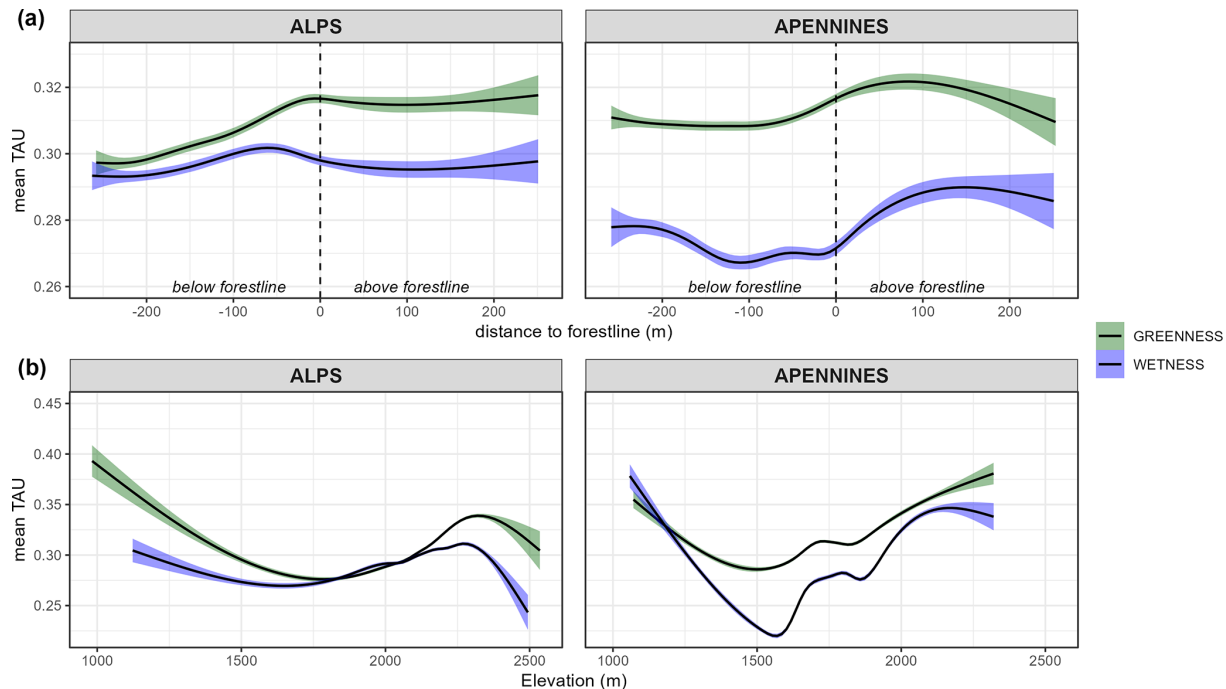
Figure 8. Wetness (blue) and greenness (green) GAM functions with a level of confidence of 0.95, according to the elevation **(a)** and to the distance to the forestline **(b)** in the Alps (left) and in the Apennines (right). We considered the mean values of each forestline buffer. The models are not statistically significant ($\alpha > 0.05$).

5 Conclusions

This study proposes a novel method to demarcate at a regional scale the upper forestlines in geographic areas where the climatic treeline threshold (i.e., the 6 °C isotherm sensu Körner and Paulsen, 2004) can not be matched. We introduced several parameters to define only the forestlines closest to their potential position, detecting the ones nearest to mountain tops with land cover and bioclimatic features. The use of TCD, with national or European digital terrain models, makes this method applicable in most parts of Europe, but with similar datasets also in other world regions and at a different scale of analysis. High spatial resolution, wide geographical coverage, and open data availability policies are important issues for the replicability of the algorithm and for ensuring the quality of both the detection results and the trend analysis. Landsat images permit analyzing 40-year-long time series with a suitable spatial resolution. Even though the two types of indices have different targets (greenness indices for photosynthetic activity and wetness indices for water content), the results were congruous and emphasized the altitudinal expansion of the forestline ecotone at national scale. Wetness indices were more sensitive in areas with denser canopy cover, probably due to gap-filling processes and increasing biomass. Greenness indices detected more relevant trends, especially in areas with sparse or medium canopy cover, probably where recent tree encroachment occurred in previously open areas.

In the current context of climate change and post-abandonment successional dynamics, the implementation of semi-automatic methods for the detection and monitoring of vegetation spatial patterns and modeling of its spectral trends is definitely an added value. With this study, by different spectral indices, we detected hotspots of changes, and we put grounds for future landscape-scale analyses aimed at better assessing the relationships between climate, topography, vegetation dynamics, and forest structure changes.

Appendix A

Table A1. Selected Italian GMBA mountain groups, whose peaks having land cover and thermotypes suitable for the proposed algorithm. Elevation information was extracted from the Tinitaly DEM, limiting the areas to the national administrative boundaries.

ID		Mountain group statistics				Forestline statistics					
Code	Name	Highest peak (m)	Min elevation (m)	Forested area (km²)	Area (km²)	Length (km)	Mean length (km)	No.	Mean elevation (m)	Median elevation (m)	Max elevation (m)	Length/forested area (km km⁻²)
Alps											
ADPA	Adamello–Presanella Alps	3552	250	657	1379	115	0.98 ± 0.56	118	2196 ± 27	2196	2343	0.175
BA	Bergamasque Alps	3030	198	815	1417	151	1.06 ± 0.74	146	2179 ± 39	2176	2332	0.185
BER	Bernina Range	3998	0	431	976	76	1.13 ± 0.78	67	2233 ± 46	2219	2416	0.176
BG	Brenta group	3163	190	455	706	68	1.19 ± 0.97	57	2107 ± 37	2102	2272	0.149
BLP	Bellunese Prealps	2457	26	1058	1494	128	1.76 ± 2.62	73	1701 ± 60	1695	1889	0.121
BSP	Brescia Prealps	2250	125	811	1124	96	2.16 ± 1.59	44	1892 ± 48	1886	2109	0.118
CAA	Carnic Alps	2778	241	1202	1720	173	1.36 ± 1.38	92	2049 ± 51	2042	2193	0.144
CGA	Central Graian Alps	3747	660	136	619	26	1.09 ± 0.6	24	2329 ± 37	2321	2479	0.191
COA	Cottian Alps	3286	0	345	823	69	1.08 ± 0.67	64	2295 ± 51	2285	2481	0.2
COP	Como Prealps	2242	0	569	847	78	3.12 ± 3.62	25	1773 ± 82	1759	1950	0.137
CP	Carnic Prealps	2703	132	933	1304	125	2.21 ± 3.1	78	1899 ± 55	1892	2092	0.134
FD	Fiemme Dolomites	2844	186	1445	1971	219	1.56 ± 1.4	141	2140 ± 40	2134	2326	0.151
GCA	Grand Combin Alps	3725	555	141	538	29	1.14 ± 0.8	82	2293 ± 38	2287	2420	0.206
GCC	Gruppo Camino-Concarena	2547	158	1373	2003	164	1.51 ± 1.62	106	1833 ± 63	1819	2126	0.119
GP	Garda Prealps	2251	12	1273	1686	168	1.87 ± 1.72	90	1911 ± 76	1897	2163	0.132
GPM	Grand Paradis Massif	4060	236	537	1563	93	1.01 ± 0.61	29	2299 ± 45	2291	2491	0.174
JA	Julian Alps	2751	311	286	439	48	1.17 ± 0.64	41	1819 ± 47	1811	2017	0.168
LGA	Ligurian Alps	2650	0	1503	2051	169	1.88 ± 1.58	90	2008 ± 78	1994	2262	0.112
LHMA	Lanzo and Haute Maurienne Alps	3676	0	611	1291	114	1.5 ± 1.5	76	2177 ± 56	2169	2387	0.186
LP	Ligurian Prealps	1743	0	875	1043	50	2.65 ± 5.04	19	1474 ± 109	1452	1743	0.057
LR	Livigno Range	3436	0	180	630	28	1.01 ± 0.64	26	2303 ± 26	2301	2376	0.153
MCA	Mont Cenis Alps	3468	515	126	352	27	0.84 ± 0.6	26	2325 ± 37	2320	2444	0.216
MGA	Montgenevre Alps	3301	277	797	1432	159	1.31 ± 1.21	121	2339 ± 41	2332	2500	0.2
MLSGA	Mont Leone and Saint Gothard Alps	3551	0	132	379	21	1.51 ± 1.13	18	2157 ± 28	2153	2245	0.159
MRA	Monte Rosa Alps	4607	197	584	1382	113	1.75 ± 1.38	110	2275 ± 51	2266	2469	0.194
MVA	Monte Viso Alps	3841	275	1041	1971	192	1.32 ± 1.28	86	2282 ± 50	2277	2486	0.185
MWA	Mischabel and Weissmies Alps	3610	223	194	392	42	1.02 ± 0.58	41	2127 ± 48	2119	2313	0.216
NED	Northeastern Dolomites	3261	529	744	1474	118	1.11 ± 0.72	108	2158 ± 26	2154	2253	0.159
NG	Nonsberg Group	2953	200	693	966	119	1.61 ± 1.33	72	2181 ± 41	2180	2319	0.172
NWD	Northwest Dolomites	3343	276	803	1426	156	1.11 ± 0.74	141	2190 ± 29	2188	2298	0.194
ORT	Ortler Alps	3892	270	715	1768	123	1.28 ± 0.9	99	2293 ± 36	2287	2419	0.172
OTZ	Ötztal Alps	3723	0	300	1024	51	0.97 ± 0.61	53	2323 ± 30	2319	2438	0.171
PSM	Pale di San Martino	3190	260	456	742	74	1.8 ± 2.05	40	2064 ± 55	2060	2263	0.161
PV	Puster Valley	3424	807	257	531	61	1.08 ± 0.7	56	2202 ± 19	2200	2288	0.236

Table A1. Continued.

| ID		Mountain group statistics				Forestline statistics						
Code	Name	Highest peak (m)	Min elevation (m)	Forested area (km^2)	Area (km^2)	Length (km)	Mean length (km)	No.	Mean elevation (m)	Median elevation (m)	Max elevation (m)	Length/forested area (km km^{-2})
SA	Sarntal Alps	2773	239	654	1115	124	1.28 ± 0.86	97	2119 ± 29	2110	2245	0.19
SED	Southeast Dolomites	3217	351	446	659	54	1.52 ± 1.09	34	2050 ± 51	2041	2217	0.12
STA	Stubai Alps	3454	675	123	355	23	1.01 ± 0.66	23	2125 ± 34	2118	2251	0.189
SVA	Southern Valais Alps	2590	193	995	1412	155	2.34 ± 2.31	66	1953 ± 105	1927	2396	0.156
SVR	Sesvenna Range	3174	0	120	359	17	0.96 ± 0.43	19	2275 ± 22	2271	2370	0.141
TVA	Ticino and Verbano Alps	3272	192	603	898	138	1.58 ± 1.48	87	2098 ± 57	2093	2335	0.229
VAP	Varese Prealps	1648	0	313	410	16	2.31 ± 2.44	7	1424 ± 70	1417	1603	0.052
VIP	Vicentine Prealps	2333	34	1916	2843	175	2.24 ± 3.66	78	1917 ± 57	1907	2135	0.091
WMA	Weisshorn and Matterhorn Alps	4470	448	122	424	22	0.97 ± 0.72	23	2340 ± 35	2336	2458	0.183
ZA	Zillertal Alps	3499	563	381	863	52	0.81 ± 0.31	64	2186 ± 22	2186	2249	0.136
Apennines												
AL	Alburni	1897	0	1699	2277	43	3.09 ± 3.2	14	1643 ± 91	1622	1886	0.025
APUA	Apuan Alps	1937	0	965	1224	96	2.34 ± 3	41	1484 ± 111	1468	1864	0.099
CAAP	Central Abruzzi Apennines	1999	387	559	887	65	2.61 ± 3.44	22	1746 ± 42	1742	1862	0.117
GS	Gran Sasso	2908	90	815	1795	80	1.86 ± 1.48	43	1751 ± 61	1738	1964	0.098
LA	Laga	2457	90	1066	1662	132	3.15 ± 4.27	42	1782 ± 48	1778	1989	0.124
MA	Matese	2049	60	810	1211	67	2.58 ± 2.66	26	1651 ± 56	1641	1820	0.083
MJ	Majella	2792	98	766	1344	65	2.25 ± 3.83	29	2124 ± 106	2118	2383	0.085
MM	Monti Marsicani	2284	325	507	943	72	1.63 ± 1.77	44	1941 ± 35	1935	2066	0.142
MR	Monti Reatini	2214	369	275	389	47	1.63 ± 1.12	29	1773 ± 38	1768	1906	0.172
MS	Monti Sibillini	2476	239	409	871	68	1.89 ± 2.11	36	1692 ± 48	1686	1902	0.166
MSE	Monti Simbruini-Ernici	2155	223	811	1034	98	2.57 ± 2.28	38	1818 ± 40	1813	1977	0.12
PO	Pollino	2265	0	1287	3326	107	6.66 ± 11.52	16	1910 ± 88	1915	2147	0.083
SVE	Sirente Velino	2484	248	426	1069	78	1.62 ± 1.56	53	1904 ± 39	1897	2101	0.182
TEA	Tuscan Emilian Apennines	2163	20	4387	6245	345	2.85 ± 5.46	121	1667 ± 45	1664	1808	0.079
TRA	Tosco Romagnolo Apennines	1654	47	3954	5659	28	1.85 ± 2.01	15	1301 ± 47	1286	1427	0.007
WAA	Western Abruzzi Apennines	2247	35	1142	1664	154	2.49 ± 2.62	62	1844 ± 43	1839	2045	0.135

Appendix B
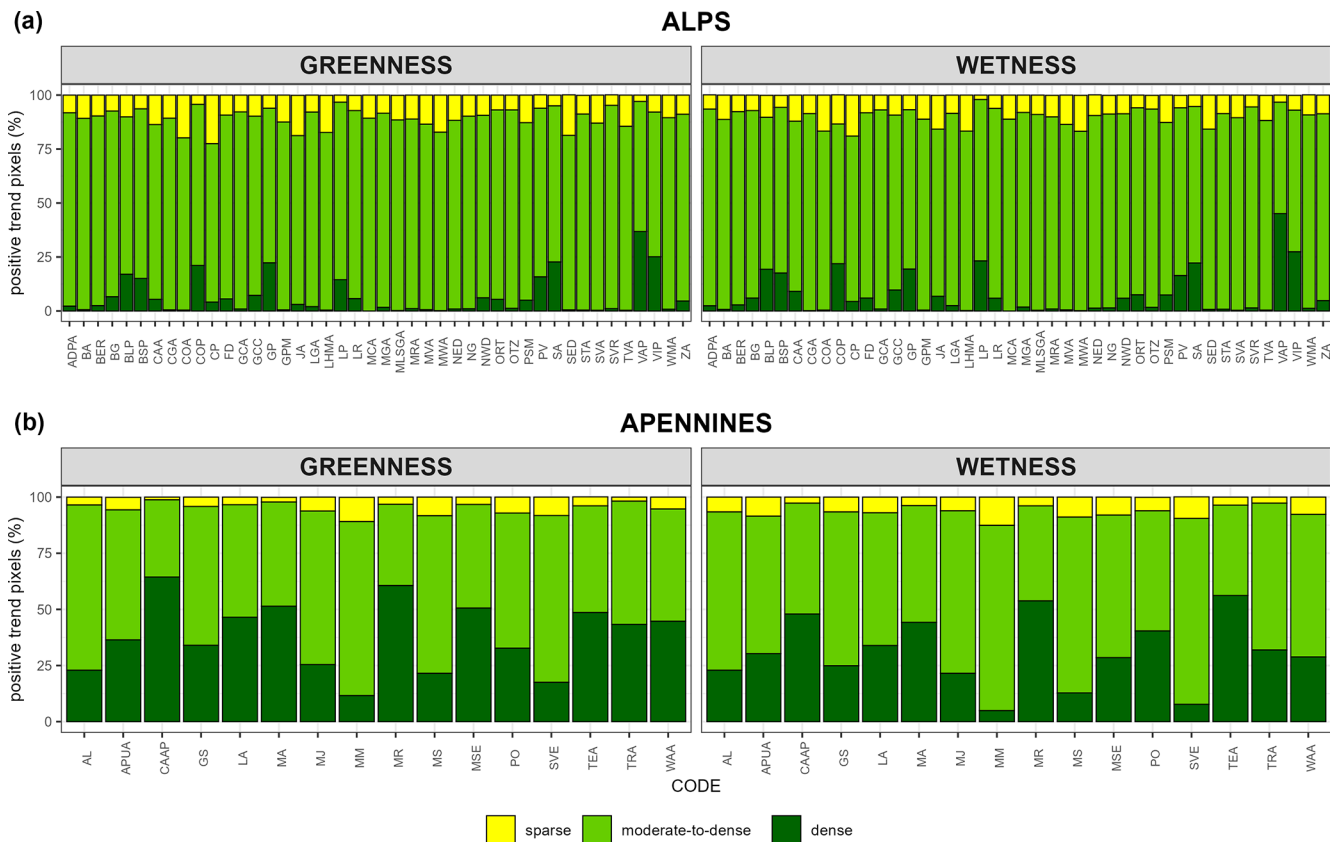
Figure B1. Percentage of highly significant positive greenness (left panels) and wetness (right panels) trend pixels of each tree cover density class in GMBA mountain groups of the Alps **(a)** and the Apennines **(b)**. Code explanations are in Table A1 (Appendix A).

References

Ameztegui, A., Coll, L., Brotons, L., and Ninot, J. M.: Land-use legacies rather than climate change are driving the recent upward shift of the mountain tree line in the Pyrenees, Global Ecol. Biogeogr., 25, 263–273, https://doi.org/10.1111/geb.12407, 2016.

Anselmetto, N., Sibona, E. M., Meloni, F., Gagliardi, L., Bocca, M., and Garbarino, M.: Land Use Modeling Predicts Divergent Patterns of Change Between Upper and Lower Elevations in a Subalpine Watershed of the Alps, Ecosystems, 25, 1295–1310, https://doi.org/10.1007/s10021-021-00716-7, 2022.

Arekhi, M., Yesil, A., Ozkan, U. Y., and Balik Sanli, F.: Detecting treeline dynamics in response to climate warming using forest stand maps and Landsat data in a temperate forest, Forest Ecosystems, 5, 23, https://doi.org/10.1186/s40663-018-0141-3, 2018.

Bader, M. Y., Llambí, L. D., Case, B. S., Buckley, H. L., Toivonen, J. M., Camarero, J. J., Cairns, D. M., Brown, C. D., Wiegand, T., and Resler, L. M.: A global framework for linking alpine-treeline ecotone patterns to underlying processes, Ecography, 44, 265–292, https://doi.org/10.1111/ecog.05285, 2021.

Bayle, A., Gascoin, S., Berner, L. T., and Choler, P.: Landsat-based greening trends in alpine ecosystems are inflated by multidecadal increases in summer observations, Ecography, 2024, e07394, https://doi.org/10.1111/ecog.07394, 2024.

Bayle, A., Nicoud, B., Mansons, J., Francon, L., Corona, C., and Choler, P.: Alpine greening deciphered by forest stand and structure dynamics in advancing treelines of the southwestern European Alps, Remote Sens. Ecol. Conserv., https://doi.org/10.1002/rse2.430, 2025.

Bengtsson, H.: A Unifying Framework for Parallel and Distributed Processing in R using Futures, R J., 13, 208–227, https://doi.org/10.32614/RJ-2021-048, 2021.

Berdanier, A.: Global treeline position, Nature Education Knowledge, 3, 11–19, 2010.

Bharti, R. R., Adhikari, B. S., and Rawat, G. S.: Assessing vegetation changes in timberline ecotone of Nanda Devi National Park, Uttarakhand, Int. J. Appl. Earth Obs. Geoinformation, 18, 472–479, https://doi.org/10.1016/j.jag.2011.09.018, 2012.

Blasi, C., Capotorti, G., Copiz, R., Guida, D., Mollo, B., Smiraglia, D., and Zavattero, L.: Classification and mapping of the ecoregions of Italy, Plant Biosyst., 148, 1255–1345, https://doi.org/10.1080/11263504.2014.985756, 2014.

Bolton, D. K., Coops, N. C., Hermosilla, T., Wulder, M. A., and White, J. C.: Evidence of vegetation greening at alpine treeline ecotones: Three decades of Landsat spectral trends informed by lidar-derived vertical structure, Environ. Res. Lett., 13, 084022, https://doi.org/10.1088/1748-9326/aad5d2, 2018.

Bonanomi, G., Rita, A., Allevato, E., Cesarano, G., Saulino, L., di Pasquale, G., Allegrezza, M., Pesaresi, S., Borghetti, M., Rossi, S., and Saracino, A.: Anthropogenic and environmental factors affect the tree line position of Fagus sylvatica along the Apennines (Italy), J. Biogeogr., 45, 2595–2608, https://doi.org/10.1111/jbi.13408, 2018.

Bonanomi, G., Zotti, M., Mogavero, V., Cesarano, G., Saulino, L., Rita, A., Tesei, G., Allegrezza, M., Saracino, A., and All-evato, E.: Climatic and anthropogenic factors explain the variability of Fagus sylvatica treeline elevation in fifteen mountain groups across the Apennines, Forest Ecosystems, 7, 5, https://doi.org/10.1186/s40663-020-0217-8, 2020.

Bonanomi, G., Mogavero, V., Rita, A., Zotti, M., Saulino, L., Tesei, G., Allegrezza, M., Saracino, A., Rossi, S. and Allevato, E.: Shrub facilitation promotes advancing of the Fagus sylvatica treeline across the Apennines (Italy), Journal of Vegetation Sciences, 32, e13054, https://doi.org/10.1111/jvs.13054, 2021.

Brown, F. C., Brumby, S. P., Guzder-Williams, B., Birch, T., Hyde, S., Mazzariello, J., Czerwinski, W., Pasquarella, V. J., Haertel, R., Ilyushchenko, S., Schwehr, K., Weisse, M., Stolle, F., Hanson, C., Guinan, O., Moore, R., and Tait, A. M.: DynamicWorld, Near real-time global 10m land use land cover mapping, [data set], Scientific Data, 9, 251, https://doi.org/10.1038/s41597-022-01307-4, 2022.

Caccianiga, M., Andreis, C., Armiraglio, S., Leonelli, G., Pelfini, M., and Sadla, D.: Climate continentality and treeline species distribution on the Alps, Plant Biosystems - An International Journal Dealing with all Aspects of Plant Biology, 142, 66–78, https://doi.org/10.1080/11263500701872416, 2008.

Camps-Valls, G., Campos-Taberner, M., Moreno-Martinez, Á., Walther, S., Duveiller, G., Cescatti, A., Mahecha, M. D., Muñoz-Marí J., García-Haro, F. J., Guanter, L., Jung, M., Gamon, J. A., Reichstein, M. and Running, S. W. : A unified vegetation index for quantifying the terrestrial biosphere, Science Advances, 7, eabc7447, https://doi.org/10.1126/sciadv.abc7447, 2021

Carlson, B. Z., Corona, M. C., Dentant, C., Bonet, R., Thuiller, W., and Choler, P.: Observed long-term greening of alpine vegetation – A case study in the French Alps, Environ. Res. Lett., 12, 114006, https://doi.org/10.1088/1748-9326/aa84bd, 2017.

Chhetri, P. K. and Thai, E.: Remote sensing and geographic information systems techniques in studies on treeline ecotone dynamics, J. Forestry Res., 30, 1543–1553, https://doi.org/10.1007/s11676-019-00897-x, 2019.

Choler, P., Bayle, A., Carlson, B. Z., Randin, C., Filippa, G., and Cremonese, E.: The tempo of greening in the European Alps: Spatial variations on a common theme, Glob. Change Biol., 27, 5614–5628, https://doi.org/10.1111/gcb.15820, 2021.

Choler, P., Bayle, A., Fort, N., and Gascoin, S.: Waning snowfields have transformed into hotspots of greening within the alpine zone, Nat. Clim. Change, 15, 80–85, https://doi.org/10.1038/s41558-024-02177-x, 2024.

Cohen, W. B. and Goward, S.: Landsat's role in ecological applications of remote sensing, Bioscience, 54, 535–545, https://doi.org/10.1641/0006-3568(2004)054[0535:LRIEAO]2.0.CO;2, 2004.

Cohen W. B., Spies T., and Fiorella M.: Estimating the age and structure of forests in a multi-ownership landscape of western Oregon, U.S.A. Int. J. Remote Sens., 16, 721–746, https://doi.org/10.1080/01431169508954436, 1995.

Compostella, C. and Caccianiga, M.: A comparison between different treeline types shows contrasting responses to climate fluctuations, Plant Biosyst., 151, 436–449, https://doi.org/10.1080/11263504.2016.1179695, 2017.

Copernicus Land Monitoring Service:Tree Cover Density 2018 - Present (raster 10m), Europe, yearly, Nov. 2024. European Environment Agency, [data set], https://doi.org/10.2909/e677441e-fb94-431c-b4f9-304f10e4dfd8, 2024.

Crist, E. P.: A TM Tasseled Cap equivalent transformation for reflectance factor data, Remote Sens. Environ., 17, 301–306, https://doi.org/10.1016/0034-4257(85)90102-6, 1985.

Crist, E. P. and Cicone, R. C.: A Physically-Based Transformation of Thematic Mapper Data - The TM Tasseled Cap, IEEE Transactions on Geoscience and Remote Sensing, 22, 256–263, 1984.

Csárdi G. and Chang W.: callr: Call R from R R package version 3.7.6, CRAN [code], https://CRAN.R-project.org/package=callr (last access: 28 February 2025), 2024.

Debussche, M., Lepart, J., and Dervieux, A.: Mediterranean landscape changes: Evidence from old postcards, Global Ecol. Biogeogr., 8, 3–15, https://doi.org/10.1046/j.1365-2699.1999.00316.x, 1999.

Diàz-Varela, R. A., Colombo, R., Meroni, M., Calvo-Iglesias, M., S., Buffoni, A., and Tagliaferri, A.: Spatio-temporal analysis of alpine ecotones: A spatial explicit model targeting altitudinal vegetation shifts, Ecol. Modell., 221, 621–633, https://doi.org/10.1016/j.ecolmodel.2009.11.010, 2010.

Dziomber, L., Gobet, E., Leunda, M., Gurtner, L., Vogel, H., Tournier, N., Damanik, A., Szidat, S., Tinner, W., and Schwörer, C.: 3 Palaeoecological multiproxy reconstruction captures long-term climatic and anthropogenic impacts on vegetation dynamics in the Rhaetian Alps, Rev. Palaeobot. Palyno., 321, 105020, https://doi.org/10.1016/J.REVPALBO.2023.105020, 2024.

EEA: Copernicus Land Monitoring Service – High Resolution Layer – Tree Cover & Forests, Product User Manual (PUM), https://land.copernicus.eu/en/technical-library/product-user-manual-tree-cover-and-forests-2018-2021, 2025.

FAO: Global Forest Resources Assessment (FRA),FAO forestry paper 140, Food and Agriculture Organization of the United Nations, Rome, 2000.

Fauquette, S., Suc, J.-P., Médail, F., Muller, S. D., Jiménez-Moreno, G., Bertini, A., Martinetto, E., Popescu, S. M., Zheng, Z., and de Beaulieu, J.-L.: The Alps: A Geological, Climatic and Human Perspective on Vegetation History and Modern Plant Diversity, Mountains, Climate and Biodiversity, https://amu.hal.science/hal-01888883 (last access: 28 February 2025), 2018.

Fissore, V., Motta, R., Palik, B., and Mondino, E. B.: The role of spatial data and geomatic approaches in treeline mapping: A review of methods and limitations, Eur. J. Remote Sens., 48, 777–792, https://doi.org/10.5721/EuJRS20154843, 2015.

Flood, N.: Seasonal Composite Landsat TM/ETM+ Images Using the Medoid (a Multi-Dimensional Median), Remote Sensing, 5, 6481–6500, https://doi.org/10.3390/rs5126481, 2013.

Foster, D. R., Motzkin, G. and Slater, B.: Land-Use History as Long-Term Broad-Scale Disturbance: Regional Forest Dynamics in Central New England, Ecosystems 1, 96–119, https://doi.org/10.1007/s100219900008, 1998.

Gao, B.-C.: NDWI – A normalized difference water index for remote sensing of vegetation liquid water from space, Remote Sens. Environ., 58, 257–266, https://doi.org/10.1016/S0034-4257(96)00067-3, 1996.

Garbarino, M., Morresi, D., Urbinati, C., Malandra, F., Motta, R., Sibona, E. M., Vitali, A, and Weisberg, P. J.: Contrasting land use legacy effects on forest landscape dynamics in the Italian Alps and the Apennines, Landscape Ecol., 35, 2679–2694, https://doi.org/10.1007/s10980-020-01013-9, 2020.

Garbarino, M., Morresi, D., Anselmetto, N., and Weisberg, P. J.: Treeline remote sensing: from tracking treeline shifts to multi-dimensional monitoring of ecotonal change, Remote Sensing in Ecology and Conservation, 9, 729–742, https://doi.org/10.1002/rse2.351, 2023.

García, M. J. L. and Caselles, V.: Mapping burns and natural reforestation using thematic mapper data, Geocarto Int., 6, 31–37, https://doi.org/10.1080/10106049109354290, 1991.

Gilles, A., Lavergne, S., and Carcaillet, C.: Unsuspected prevalence of Pinus cembra in the high-elevation sky islands of the western Alps, Plant Ecol., 224, 865–873, https://doi.org/10.1007/s11258-023-01341-1, 2023.

Gómez, C., White, J. C., and Wulder, M. A.: Characterizing the state and processes of change in a dynamic forest environment using hierarchical spatio-temporal segmentation, Remote Sens. Environ., 115, 1665–1679, https://doi.org/10.1016/j.rse.2011.02.025, 2011.

Gómez, C., White, J. C., and Wulder, M. A.: Optical remotely sensed time series data for land cover classification: A review, ISPRS J. Photogramm., 116, 55–72, https://doi.org/10.1016/J.ISPRSJPRS.2016.03.008, 2016.

Hansson, A., Dargusch, P., and Shulmeister, J.: A Review of Methods Used to Measure Treeline Migration and Their Application, Journal of Environmental Informatics Letters, 4, 1–10, https://doi.org/10.3808/jeil.202000037, 2020.

Hansson, A., Yang, W. H., Dargusch, P., and Shulmeister, J.: Investigation of the Relationship Between Treeline Migration and Changes in Temperature and Precipitation for the Northern Hemisphere and Sub-regions, Current Forestry Reports, 9, 72–100, https://doi.org/10.1007/s40725-023-00180-7, 2023.

Harsch, M. A. and Bader, M. Y.: Treeline form – a potential key to understanding treeline dynamics, Global Ecol. Biogeogr., 20, 582–596, https://doi.org/10.1111/j.1466-8238.2010.00622.x, 2011.

Hastie, T. J. and Tibshirani, R. J.: Generalized Additive Models, Chapman & Hall/CRC, ISBN 978-0-412-34390-2, 1990.

He, X., Jiang, X., Spracklen, D. v., Holden, J., Liang, E., Liu, H., Xu, C., Du, J., Zhu, K., Elsen, P. R., and Zeng, Z.: Global distribution and climatic controls of natural mountain treelines, Glob. Change Biol., 29, 7001–7011, https://doi.org/10.1111/gcb.16885, 2023.

Hijmans, R.: terra: Spatial Data Analysis, R package version 1.7-55, CRAN [code], https://CRAN.R-project.org/package=terra (last access: 28 February 2025), 2023.

Holtmeier, F. K.: Mountain Timberlines, Adv. Global Change Res., 36, 1–4, https://doi.org/10.1007/978-1-4020-9705-8_1, 2009.

Holtmeier, F. K. and Broll, G.: Sensitivity and response of northern hemisphere altitudinal and polar treelines to environmental change at landscape and local scales, Global Ecol. Biogeogr., 14, 395–410, https://doi.org/10.1111/j.1466-822X.2005.00168.x, 2005.

Holtmeier, F. K. and Broll, G.: Treeline research-from the roots of the past to present time. a review, Forests, 11, 38, https://doi.org/10.3390/f11010038, 2020.

Huete, A., Didan, K., Miura, T., Rodriguez, E. P., Gao, X., and Ferreira, L. G.: Overview of the radiometric and biophysical performance of the MODIS vegetation indices, Remote Sens. Environ., 83, 195–213, https://doi.org/10.1016/S0034-4257(02)00096-2, 2002.

Huete, A. R.: Vegetation Indices, Remote Sensing and Forest Monitoring, Geography Compass, 6, 513–532, https://doi.org/10.1111/j.1749-8198.2012.00507.x, 2012.

Isotta, F. A., Frei, C., Weilguni, V., Perčec Tadić, M., Lassègues, P., Rudolf, B., Pavan, V., Cacciamani, C., Antolini, G., Ratto, S. M., Munari, M., Micheletti, S., Bonati, V., Lussana, C., Ronchi, C., Panettieri, E., Marigo, G., and Vertačnik, G.: The climate of daily precipitation in the Alps: Development and analysis of a high-resolution grid dataset from pan-Alpine rain-gauge data, Int. J. Climatol., 34, 1657–1675, https://doi.org/10.1002/joc.3794, 2014.

Kauth R. J. and G. S. Thomas: The Tasselled Cap – A Graphic Description of the Spectral-Temporal Development of Agricultural Crops as Seen by LANDSAT, in: Proceedings of the Symposium on Machine Processing of Remotely Sensed Data, University of West Lafayette, Indiana, 29 June 29–1 July, 1976.

Körner, C.: Alpine Ecosystems and the High-Elevation Treeline, Encyclopedia of Ecology, 138–144, https://doi.org/10.1016/B978-008045405-4.00314-1, 2008.

Körner, C.: Alpine Treelines, in: Functional Ecology of the Global High Elevation Tree Limits, Springer, https://doi.org/10.1007/978-3-0348-0396-0, 2012.

Körner, C. and Paulsen, J.: A world-wide study of high altitude treeline temperatures, J. Biogeogr., 31, 713–732, https://doi.org/10.1111/j.1365-2699.2003.01043.x, 2004.

Kumar, R., Nath, A. J., Nath, A., Sahu, N., and Pandey, R.: Landsat-based multi-decadal spatio-temporal assessment of the vegetation greening and browning trend in the Eastern Indian Himalayan Region, Remote Sensing Applications: Society and Environment, 25, 100695, https://doi.org/10.1016/j.rsase.2022.100695, 2022.

Lang, N., Jetz, W., Schindler, K., and Wegner, J. D.: A high-resolution canopy height model of the Earth, Nature Ecology and Evolution, 7, 1778–1789, https://doi.org/10.1038/s41559-023-02206-6, 2023.

Leonelli, G., Pelfini, M., and Di Cella, U.: Detecting climatic treelines in the Italian alps: The influence of geomorphological factors and human impacts, Phys. Geogr., 30, 338–352, https://doi.org/10.2747/0272-3646.30.4.338, 2009.

Lingua, E., Cherubini, P., Motta, R., and Nola, P.: Spatial structure along an altitudinal gradient in the Italian central Alps suggests competition and facilitation among coniferous species, J. Veg. Sci. 19, 425–436, 2008.

Malandra, F., Vitali, A., Urbinati, C., Weisberg, P. J., and Garbarino, M.: Patterns and drivers of forest landscape change in the Apennines range, Italy, Reg. Environ. Change, 19, 1973–1985, https://link.springer.com/article/10.1007/s10113-019-01531-6, 2019.

Malanson, G. P., Resler, L. M., Bader, M. Y., Holtmeier, F. K., Butler, D. R., Weiss, D. J., Daniels, L. D., and Fagre, D. B.: Mountain treelines: A roadmap for research orientation, Arct. Antarct. Alp. Res., 43, 167–177, https://doi.org/10.1657/1938-4246-43.2.167, 2011.

McCune, B.: Improved estimates of incident radiation and heat load using non-parametric regression against topographic variables, J. Veg. Sci. 18, 751–754, 2007.

McManus, K. M., Morton, D. C., Masek, J. G., Wang, D., Sexton, J. O., Nagol, J. R., Ropars, P., and Boudreau, S.: Satellite-based evidence for shrub and graminoid tundra expansion in northern Quebec from 1986 to 2010, Glob. Change Biol., 18, 2313–2323, https://doi.org/10.1111/j.1365-2486.2012.02708.x, 2012.

Morales-Molino, C., Leunda, M., Morellón, M., Gardoki, J., Ezquerra, F. J., Muñoz Sobrino, C., Rubiales, J. M., and Tinner, W.: Millennial land use explains modern high-elevation vegetation in the submediterranean mountains of Southern Europe, J. Biogeogr., 49, 1779–1792, https://doi.org/10.1111/jbi.14472, 2022.

Morley, P. J., Donoghue, D. N. M., Chen, J. C., and Jump, A. S.: Integrating remote sensing and demography for more efficient and effective assessment of changing mountain forest distribution, Ecol. Inform., 43, 106–115, https://doi.org/10.1016/j.ecoinf.2017.12.002, 2018.

Morley, P. J., Donoghue, D. N. M., Chen, J. C., and Jump, A. S.: Quantifying structural diversity to better estimate change at mountain forest margins, Remote Sens. Environ., 223, 291–306, https://doi.org/10.1016/J.RSE.2019.01.027, 2019.

Morresi, D., Vitali, A., Urbinati, C., and Garbarino, M.: Forest spectral recovery and regeneration dynamics in stand-replacing wildfires of central Apennines derived from Landsat time series, Remote Sensing, 11, 308, https://doi.org/10.3390/rs11030308, 2019.

Motta, R., Morales, M., and Nola, P.: Human land-use, forest dynamics and tree growth at the treeline in the Western Italian Alps, Ann. For. Sci., 63, 739–747m https://doi.org/10.1051/forest:2006055, 2006.

Neeti, N. and Eastman, J. R.: A Contextual Mann-Kendall Approach for the Assessment of Trend Significance in Image Time Series, T. GIS, 15, 599–611, https://doi.org/10.1111/j.1467-9671.2011.01280.x, 2011.

Nguyen, T. A., Rußwurm, M., Lenczner, G., and Tuia, D.: Multi-temporal forest monitoring in the Swiss Alps with knowledge-guided deep learning, Remote Sens. Environ., 305, 114109, https://doi.org/10.1016/j.rse.2024.114109, 2024

Obojes, N., Buscarini, S., Meurer, A. K., Tasser, E., Oberhuber, W., Mayr, S., and Tappeiner, U.: Tree growth at the limits: the response of multiple conifers to opposing climatic constraints along an elevational gradient in the Alps, Frontiers in Forests and Global Change, 7, https://doi.org/10.3389/ffgc.2024.1332941, 2024.

Pecher, C., Tasser, E., and Tappeiner, U.: Definition of the potential treeline in the European Alps and its benefit for sustainability monitoring, Ecol. Indic., 11, 438–447, https://doi.org/10.1016/j.ecolind.2010.06.015, 2011.

Pesaresi, S., Biondi, E., and Casavecchia, S.: Bioclimates of italy, J. Maps [data set], 13, 955–960, https://doi.org/10.1080/17445647.2017.1413017, 2017.

Piermattei, A., Garbarino, M., and Urbinati, C.: Structural attributes, tree-ring growth and climate sensitivity of Pinus nigra Arn. at high altitude: common patterns of a possible treeline shift in the central Apennines (Italy), Dendrochronologia, 32, 210–219, https://doi.org/10.1016/J.DENDRO.2014.05.002, 2014.

Piermattei, A., Lingua, E., Urbinati, C., and Garbarino, M.: Pinus nigra anthropogenic treelines in the central Apennines show common pattern of tree recruitment, Eur. J. For. Res., 135, 1119–1130, https://doi.org/10.1007/s10342-016-0999-y, 2016.

Piper, F. I., Viñegla, B., Linares, J. C., Camarero, J. J., Cavieres, L. A., and Fajardo, A.: Mediterranean and temperate treelines are controlled by different environmental drivers, J. Ecol., 104, 691–702, https://doi.org/10.1111/1365-2745.12555, 2016.

Potapov, P., Li, X., Hernandez-Serna, A., Tyukavina, A., Hansen, M. C., Kommareddy, A., Pickens, A., Turubanova, S., Tang, H., Silva, C. E., Armston, J., Dubayah, R., Blair, J. B., and Hofton, M.: Mapping global forest canopy height through integration of GEDI and Landsat data, Remote Sens. Environ., 253, 112165, https://doi.org/10.1016/j.rse.2020.112165, 2021.

Powell, S. L., Cohen, W. B., Healey, S. P., Kennedy, R. E., Moisen, G. G., Pierce, K. B., and Ohmann, J. L.: Quantification of live aboveground forest biomass dynamics with Landsat time-series and field inventory data: A comparison of empirical modeling approaches, Remote Sens. Environ., 114, 1053–1068, https://doi.org/10.1016/j.rse.2009.12.018, 2010.

Rajala, T.: ConMK: Contextual Mann-Kendall. R package version 0.8-1, https://github.com/geoporttishare/ConMK, last access: 28 February 2025, 2024.

Rivas-Martínez, S.: Bases para una nueva clasificacion, Folia Botanica Madritensis, 10, 1–23, 1993.

Rumpf, S. B., Gravey, M., Brönnimann, O., Luoto, M., Cianfrani, C., Mariethoz, G., and Guisan, A.: From white to green: Snow cover loss and increased vegetation productivity in the European Alps, Science, 376, 1119–1122, https://doi.org/10.1126/science.abn6697, 2022.

Schroeder, T. A., Wulder, M. A., Healey, S. P., and Moisen, G. G.: Mapping wildfire and clearcut harvest disturbances in boreal forests with Landsat time series data, Remote Sens. Environ., 115, 1421–1433, https://doi.org/10.1016/J.RSE.2011.01.022, 2011.

Schultz, M., Clevers, J. G. P. W., Carter, S., Verbesselt, J., Avitabile, V., Quang, H. V., and Herold, M.: Performance of vegetation indices from Landsat time series in deforestation monitoring, Int. J. Appl. Earth Obs., 52, 318–327, https://doi.org/10.1016/j.jag.2016.06.020, 2016.

Snethlage, M. A., Geschke, J., Spehn, E. M., Ranipeta, A., Yoccoz, N. G., Körner, C., Jetz, W., Fischer, M., and Urbach, D.: A hierarchical inventory of the world's mountains for global comparative mountain science, Scientific Data [data set], 9, 149, https://doi.org/10.1038/s41597-022-01256-y, 2022a.

Snethlage, M. A., Geschke, J., Spehn, E. M., Ranipeta, A., Yoccoz, N. G., Körner, C., Jetz, W., Fischer, M., and Urbach, D.: GMBA Mountain Inventory v2, Nature Scientific Data [data set], https://doi.org/10.48601/earthenv-t9k2-1407, 2022b.

Tarquini, S., Isola, I., Favalli, M., Battistini, A., and Dotta, G.: TINITALY, a digital elevation model of Italy with a 10 meters cell size (Version 1.1), Istituto Nazionale di Geofisica e Vulcanologia (INGV) [data set], https://doi.org/10.13127/tinitaly/1.1, 2023.

Tian, L., Fu, W., Tao, Y., Li, M., and Wang, L.: Dynamics of the alpine timberline and its response to climate change in the Hengduan mountains over the period 1985–2015, Ecol. Indic., 135, 108589, https://doi.org/10.1016/j.ecolind.2022.108589, 2022.

Tolan, J., Yang, H. I., Nosarzewski, B., Couairon, G., Vo, H. V., Brandt, J., Spore, J., Majumdar, S., Haziza, D., Vamaraju, J., Moutakanni, T., Bojanowski, P., Johns, T., White, B., Tiecke, T., and Couprie, C.: Very high resolution canopy height maps from RGB imagery using self-supervised vision transformer and convolutional decoder trained on aerial lidar, Remote Sens. Environ., 300, 113888, https://doi.org/10.1016/j.rse.2023.113888, 2024.

Tucker, C. J.: Red and Photographic Infrared Linear Combinations for Monitoring Vegetation, Remote Sens. Environ., 8, 127–150, https://doi.org/10.1016/0034-4257(79)90013-0, 1979.

Vacchiano, G., Garbarino, M., Lingua, E., and Motta, R.: Forest dynamics and disturbance regimes in the Italian Apennines, Forest Ecol. Manag., 388, 57–66, https://doi.org/10.1016/j.foreco.2016.10.033, 2017.

Vitali, A., Camarero, J. J., Garbarino, M., Piermattei, A., and Urbinati, C.: Deconstructing human-shaped treelines: Microsite topography and distance to seed source control Pinus nigra colonization of treeless areas in the Italian Apennines, Forest Ecol. Manag., 406, 37–45, https://doi.org/10.1016/j.foreco.2017.10.004, 2017.

Vitali, A., Urbinati, C., Weisberg, P. J., Urza, A. K., and Garbarino, M.: Effects of natural and anthropogenic drivers on land-cover change and treeline dynamics in the Apennines (Italy), J. Veg. Sci., 29, 189–199, https://doi.org/10.1111/jvs.12598, 2018.

Wang, X. L. and Swail, V. R.: Changes of extreme Wave Heights in northern Hemisphere Oceans and related atmospheric circulation regimes, J. Climate, 14, 2204–2221, https://doi.org/10.1175/1520-0442(2001)014<2204:COEWHI>2.0.CO;2, 2001.

Wei, C., Karger, D. N., and Wilson, A. M.: Spatial detection of alpine treeline ecotones in the Western United States, Remote Sens. Environ., 240, 111672, https://doi.org/10.1016/j.rse.2020.111672, 2020.

Wickham, H., François, R., Henry, L., Müller, K., Vaughan, D.: _dplyr: A Grammar of Data Manipulation, R package version 1.1.4, CRAN [code], https://CRAN.R-project.org/package=dplyr (last access: 28 February 2025), 2023.

Wilcoxon F.: Individual comparisons by ranking methods, Biometrics, 1, 80–83, https://doi.org/10.2307/3001968, 1945.

Wood, S. N.: Fast stable restricted maximum likelihood and marginal likelihood estimation of semiparametric generalized linear models, J. R. Stat. Soc. B, 73, 3–36, https://doi.org/10.1111/j.1467-9868.2010.00749.x, 2011.

Zhou, M., Li, D., Liao, K., and Lu, D.: Integration of Landsat time-series vegetation indices improves consistency of change detection, Int. J. Digit. Earth, 16, 1276–1299, https://doi.org/10.1080/17538947.2023.2200040, 2023.

Zhu, Z.: Change detection using landsat time series: A review of frequencies, preprocessing, algorithms, and applications, ISPRS J. Photogramm., 130, 370–384, https://doi.org/10.1016/J.ISPRSJPRS.2017.06.013, 2017.

Zou, F., Tu, C., Liu, D., Yang, C., Wang, W., and Zhang, Z.: Alpine Treeline Dynamics and the Special Exposure Effect in the Hengduan Mountains, Front. Plant Sci., 13, https://doi.org/10.3389/fpls.2022.861231, 2022.